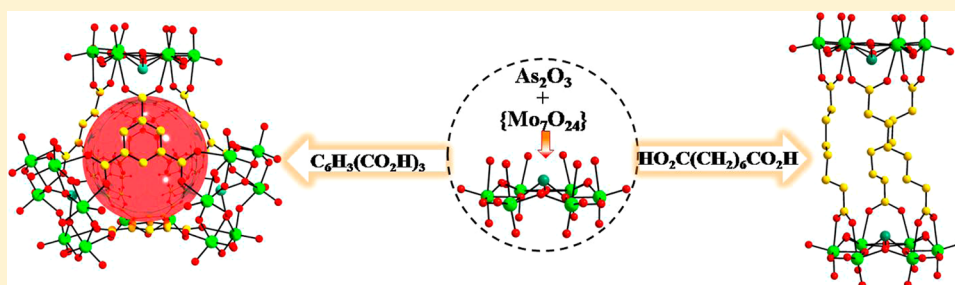


## Ligand-Directed Conformation of Inorganic–Organic Molecular Capsule and Cage

Donghui Yang,<sup>†</sup> Yanfen Liang,<sup>†</sup> Pengtao Ma,<sup>†</sup> Suzhi Li,<sup>‡</sup> Jingping Wang,<sup>\*,†</sup> and Jingyang Niu<sup>\*,†</sup><sup>†</sup>Henan Key Laboratory of Polyoxometalate, Institute of Molecular and Crystal Engineering, College of Chemistry and Chemical Engineering, Henan University, Kaifeng 475004, Henan, China<sup>‡</sup>College of Chemistry and Chemical Engineering, Engineering Research Center of Functional Material Preparation, Shangqiu Normal University, Shangqiu, 476000, Henan, China

## Supporting Information



**ABSTRACT:** Four new inorganic–organic hybrids, namely,  $(\text{NH}_4)_3\text{H}_3[\text{AsMo}_6\text{O}_{21}(\text{O}_2\text{CC}_6\text{H}_4\text{NH}_2)_3] \cdot 8.5\text{H}_2\text{O}$  (1),  $(\text{NH}_4)_{16}\text{H}_3[(\text{AsMo}_6\text{O}_{21})_3(\text{O}_2\text{CCH}_2\text{CO}_2)_5] \cdot 18\text{H}_2\text{O}$  (2),  $(\text{NH}_4)_{11}\text{H}[(\text{AsMo}_6\text{O}_{21})_2\{\text{O}_2\text{C}(\text{CH}_2)_6\text{CO}_2\}_3] \cdot 8\text{H}_2\text{O}$  (3), and  $(\text{NH}_4)_{18}\text{H}_6[(\text{AsMo}_6\text{O}_{21})_4\{\text{C}_6\text{H}_3(\text{CO}_2)_3\}_4] \cdot 24.5\text{H}_2\text{O}$  (4), were synthesized by reaction of  $\text{As}_2\text{O}_3$  with  $(\text{NH}_4)_6\text{Mo}_7\text{O}_{24} \cdot 4\text{H}_2\text{O}$  and organic components in aqueous medium. All of the four hybrids feature a common  $\{\text{AsMo}_6\}$  unit composed of a six-membered  $\text{MoO}_6$  octahedral ring capped by one  $\{\text{AsO}_3\}$  trigonal pyramid. Although these hybrids exhibit similar chemical formula, their structures are monomer, dimer (capsule), trimer, and tetramer (cage), respectively, depending upon the nature of carboxylic acids. Also, the assembly processes appear to be highly versatile and sensitive to the inherent nature of carboxylic acids, which direct the assemblies toward construction of POM clusters and participate directly to their stabilization. In addition, successful isolation of these hybrids shows that it would be possible to achieve a variety of structural predesign in this inorganic–organic system by means of a ligand design route based on the interplay between the organic molecules and polyoxometalates (POMs).

## INTRODUCTION

POMs have been known for being decorated by attaching organic molecules, which are intensely studied owing to a large variety of intriguing shapes and sizes, with remarkable properties and functions.<sup>1</sup> Covalent binding of organic components onto POMs offers several advantages and is also an important synthetic strategy for preparation of functional hybrid materials, which heightens the directionality and synergistic interaction between organic groups and POM clusters. In such respect, structural characterization of polyoxomolybdates with carboxylates has been discovered in the past two decades. Most result from amino acids or carboxylic acids combining polyoxomolybdate clusters for complex structures with varied electronic configuration and bonding patterns.<sup>2</sup> Owing to these attractive features, their syntheses are often evoked for the study of multifunctional devices. To date, a huge class of compounds, varying in their sizes, stoichiometries, and symmetries, has been synthesized and characterized.<sup>3</sup> Structures and properties of such materials depend on the nature of both the organic and the inorganic components. Thus, great efforts have been made to achieve the

rational design of the carboxylate-functionalized POMs. Generally, the architectural design principles are almost empirical, mainly according to the intuition of construction processes and phenomena, which are drastically altered by temperature, pH, ionic strength, and concentration, etc. However, it is difficult to predict the relevant geometric relationships between the POMs and the carboxylate ligands because of little directional information. In short, the formation mechanisms of POMs are not fully understood and often described as self-assembly. In this sense, control of assembly processes for affording elaborate structures from simple constituents is obviously a synthetic challenge. At present, there are few systems allowing deliberate design and subtle tuning of the POM structures.<sup>4</sup> Therefore, design of the target frameworks will open up a new avenue for generation of enormous structural variety.

Herein, we report a strategy providing ligand-accessible coordination sites to direct relevant modular assemblies in

Received: November 20, 2013

Published: February 21, 2014

constructing a new family of POM architectures. A key issue for the formation of such compounds is critically dependent on identifying carboxylic acid, which with intrinsic geometry could result in a target structure. Further, based on the different nature of carboxylic acids, four architectures derived as monomer, dimer, trimer, and tetramer (Figure 1) were isolated

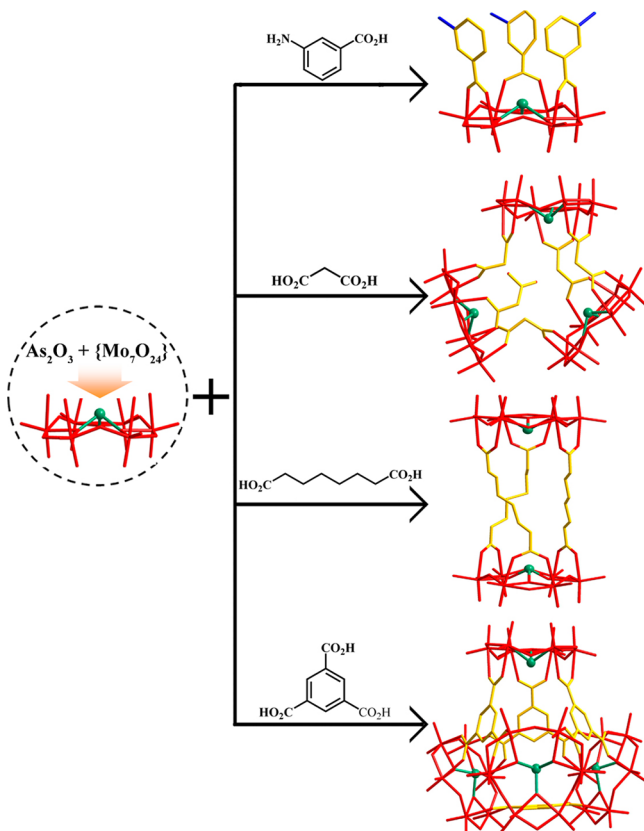


**Figure 1.** Schematic representation of the preparation of 1–4 highlighting the coordination of the carboxylate linkers. Color code: red sticks =  $\{Mo_6\}$  subunits; yellow sticks = carboxylate linkers; blue sticks = C–N; As = green spheres.

and structurally characterized in the solid state. In this work, the assembly of four compounds mentioned above yielded four architecture types:  $(NH_4)_3H_3[AsMo_6O_{21}(O_2CC_6H_4NH_2)_3] \cdot 8.5H_2O$  (1),  $(NH_4)_{16}H_3[(AsMo_6O_{21})_3(O_2CCH_2CO_2)_5] \cdot 18H_2O$  (2),  $(NH_4)_{11}H[(AsMo_6O_{21})_2\{O_2C(CH_2)_6CO_2\}_3] \cdot 8H_2O$  (3), and  $(NH_4)_{18}H_6[(AsMo_6O_{21})_4\{C_6H_3(CO_2)_3\}_4] \cdot 24.5H_2O$  (4). In particular, their dimension and composition can be stereochemically oriented and conformationally ordered by four different carboxylic acids: *m*-aminobenzoic acid ( $HO_2CC_6H_4NH_2$ ), malonic acid ( $HO_2CCH_2CO_2H$ ), suberic acid ( $HO_2C(CH_2)_6CO_2H$ ), and 1,3,5-benzenetricarboxylic acid ( $C_6H_3(CO_2H)_3$ ).

## EXPERIMENTAL SECTION

**Materials and Physical Measurements.** All chemical reagents were purchased from commercial sources and used without further purification. IR spectra were recorded on a Nicolet FT-IR 360 spectrometer using KBr pellets in the range of 4000–400  $cm^{-1}$ . C, H, and N elemental analyses were performed on a Perkin-Elmer 2400-II CHNS/O analyzer. X-ray photoelectron spectroscopy (XPS) was performed on an Axis Ultra (Kratos, U.K.) photoelectron spectroscope using monochromatic Al  $K\alpha$  (1486.7 eV) radiation. X-ray powder diffraction (XRPD) measurements were performed on a Philips

X'Pert-MPD instrument with Cu  $K\alpha$  radiation ( $\lambda = 1.54056 \text{ \AA}$ ) in the range  $2\theta = 10\text{--}40^\circ$  at 293 K. TG analyses were conducted on a Mettler-Toledo TGA/SDTA851<sup>o</sup> analyzer under the nitrogen gas atmosphere with a heating rate of 10  $^\circ C/min$  from 25 to 800  $^\circ C$ . EPR experiment of compound 2 was performed on a Bruker ER-2000-DSRC10 spectrometer at the X-band at 300 K after heating at 453 K for 7 h.

**Synthesis of 1.**  $(NH_4)_6Mo_7O_{24} \cdot 4H_2O$  (1.06 g, 0.86 mmol) was dissolved in water (15 mL); then  $As_2O_3$  (0.10 g, 0.51 mmol) and *m*-aminobenzoic acid (0.41g, 3.00 mmol) were added. The reaction mixture was stirred approximately 2 h at 70  $^\circ C$  to result in a yellow-brown solution. After cooling to room temperature, a large amount of precipitate was generated and the pH of resultant solution was 5.4. The precipitate was removed by filter. Yellow-brown block crystals of 1 were obtained by slow evaporation at room temperature after about 1 month. Yield: 0.13 g (8%) for 1 based on *m*-aminobenzoic acid. Anal. Calcd for  $C_{21}H_{50}Mo_6N_6O_{35.5}As$  (1): C, 15.71; H, 3.14; N, 5.24; Mo, 35.86; As, 4.67. Found: C, 15.19; H, 3.60; N, 5.40; Mo, 40.90; As, 5.18. IR (KBr pellet): 3429(s), 3163(s), 1627(m), 1558(s), 1453(m), 1115(w), 930(s), 918(s), 891(s), 764(s), 687(s), 669(s), 515(m), 446  $cm^{-1}$  (m).

**Synthesis of 2.** Same procedure as for 1, using 0.16 g (1.54 mmol) of malonic acid instead of *m*-aminobenzoic acid. The pH of the resultant pale yellow solution was 3.8. Yield: 0.51 g (37%) for 2 based on  $(NH_4)_6Mo_7O_{24} \cdot 4H_2O$ . Anal. Calcd for  $C_{15}H_{113}Mo_{18}N_{16}O_{101}As_3$  (2): C, 2.79; H, 2.79; N, 5.49; Mo, 42.27; As, 5.50. Found: C, 3.10; H, 3.12; N, 5.44; Mo, 46.50; As, 6.12. IR (KBr pellet): 3431(s), 3161(s), 1587(s), 1402(s), 1271(w), 933(s), 916(s), 889(s), 762(s), 678(s), 515(m), 445  $cm^{-1}$  (m).

**Synthesis of 3.** Same procedure as for 1, using 0.26 g (1.49 mmol) of suberic acid instead of *m*-aminobenzoic acid. The pH of the resultant colorless solution was 4.7. Yield: 0.18g (12%) for 3 based on suberic acid. Anal. Calcd for  $C_{24}H_{97}Mo_{12}N_{11}O_{62}As_2$  (3): C, 10.17; H, 3.45; N, 5.44; Mo, 40.64; As, 5.29. Found: C, 9.82; H, 3.93; N, 5.23; Mo, 44.20; As, 5.72. IR (KBr pellet): 3431(s), 3153(s), 1628(m), 1553(s), 1402(s), 1298(w), 930(s), 912(s), 892(s), 769(s), 689(s), 501(m), 442  $cm^{-1}$  (m).

**Synthesis of 4.**  $(NH_4)_6Mo_7O_{24} \cdot 4H_2O$  (1.06 g, 0.86 mmol) was dissolved in water (5 mL), then  $As_2O_3$  (0.10 g, 0.51 mmol) was added, and a solution of NaOH (0.12 g, 3.0 mmol) and 1,3,5-benzenetricarboxylic acid (0.21 g, 1.00 mmol) was added. After stirring at 70  $^\circ C$  for 2 h, the mixture was cooled and filtered. The pH of the resultant colorless solution was 5.7. Colorless block crystals of 4 were obtained by slow evaporation at room temperature after about 1 month. Yield: 0.46 g (33%) for 4 based on 1,3,5-benzenetricarboxylic acid. Anal. Calcd for  $C_{36}H_{139}Mo_{24}N_{18}O_{132.5}As_4$  (4): C, 7.80; H, 2.53; N, 4.55; Mo, 41.51; As 5.40. Found: C, 7.62; H, 3.18; N, 4.37; Mo, 36.50; As, 4.82. IR (KBr pellet): 3437(s), 3170(s), 1616(s), 1562(s), 1439(s), 1402(s), 1377(s), 1111(w), 935(s), 890(s), 771(s), 724(s), 680(s), 626(s), 510(m), 450  $cm^{-1}$  (m).

**X-ray Crystallography.** Intensity data were collected at 296 K on a Bruker APEX-II CCD diffractometer for 1–4 using graphite-monochromated Mo  $K\alpha$  radiation ( $\lambda = 0.71073 \text{ \AA}$ ). Routine Lorentz and polarization corrections were applied, and an absorption correction was performed using the SADABS program. Direct methods were used to solve the structure and refined by full-matrix least-squares on  $F^2$  using the SHELXTL-97 program package. Non-hydrogen atoms were refined anisotropically. Moreover,  $NH_4^+$  and lattice  $H_2O$  could not be distinguished based on electron densities, and we thus determine the lattice water molecules and  $NH_4^+$  ions by elemental analysis. CCDC reference numbers 946719–946722 for 1–4. These data can be obtained free of charge from The Cambridge Crystallographic Data Centre via [www.ccdc.cam.ac.uk/data\\_request/cif](http://www.ccdc.cam.ac.uk/data_request/cif).

## RESULTS AND DISCUSSION

**Synthesis.** In some cases, covalent grafting could allow the structural predesign of POM hybrids. Consequently, it would be of great interest to develop convenient syntheses of various

Table 1. Crystallographic Data for 1–4

	1	2	3	4
empirical formula	C <sub>21</sub> H <sub>50</sub> Mo <sub>6</sub> N <sub>6</sub> O <sub>35.5</sub> As	C <sub>15</sub> H <sub>113</sub> Mo <sub>18</sub> N <sub>16</sub> O <sub>101</sub> As <sub>3</sub>	C <sub>24</sub> H <sub>97</sub> Mo <sub>12</sub> N <sub>11</sub> O <sub>62</sub> As <sub>2</sub>	C <sub>36</sub> H <sub>139</sub> Mo <sub>24</sub> N <sub>18</sub> O <sub>132.5</sub> As <sub>4</sub>
fw	1605.12	4085.37	2833.24	5546.84
temp./K	296(2)	296(2)	296(2)	296(2)
cryst syst	triclinic	triclinic	triclinic	monoclinic
space group	P-1	P-1	P-1	C2/c
a (Å)	12.6563(17)	11.257(3)	12.066(12)	28.02(2)
b (Å)	12.8960(17)	16.412(4)	21.00(2)	23.925(16)
c (Å)	15.892(2)	30.250(8)	21.87(3)	26.979(16)
α (deg)	90.100(2)	88.947(4)	76.18(3)	90
β (deg)	107.326(2)	84.938(5)	74.673(18)	99.551(17)
γ (deg)	91.163(2)	81.281(4)	74.569(16)	90
V (Å <sup>3</sup> )	2475.5(6)	5503(2)	5066(9)	17837(21)
Z	1	2	2	4
F(000)	1545	3824	2766	10700
ρ <sub>calcd</sub> /g·cm <sup>-3</sup>	2.134	2.426	1.857	2.063
μ/mm <sup>-1</sup>	2.242	2.997	2.172	2.468
no. of reflns collected	12 612	27 367	25 125	46 926
no. of independent reflns	8656	19 136	17 509	15 630
GOOF	1.003	1.053	1.001	1.025
R(int)	0.0238	0.0470	0.0377	0.0822
final R indices (I = 2σ(I))	R <sub>1</sub> = 0.0796, ωR <sub>2</sub> = 0.2568	R <sub>1</sub> = 0.0884, ωR <sub>2</sub> = 0.2057	R <sub>1</sub> = 0.0641, ωR <sub>2</sub> = 0.1683	R <sub>1</sub> = 0.0486, ωR <sub>2</sub> = 0.1180
R indices (all data)	R <sub>1</sub> = 0.0926, ωR <sub>2</sub> = 0.2667	R <sub>1</sub> = 0.1245, ωR <sub>2</sub> = 0.2174	R <sub>1</sub> = 0.1179, ωR <sub>2</sub> = 0.1882	R <sub>1</sub> = 0.0900, ωR <sub>2</sub> = 0.1262

functionalized POMs. Among them, carboxylate groups appear to be promising candidates, which have already been used for preparation of POM hybrids. Thus far, the majority of the carboxylate-functionalized polyoxomolybdates reported in recent years are based on isopolymolybdates.<sup>2a–i,3</sup> However, compared to the hybrids based on isopolymolybdate anions, reports on heteropolymolybdate clusters are limited in the literature<sup>2j–l</sup> and the linking of heteropolymolybdates with multicarboxylic acids has remained largely unexplored.<sup>4d,e</sup> In this work, we chose (NH<sub>4</sub>)<sub>6</sub>Mo<sub>7</sub>O<sub>24</sub>·4H<sub>2</sub>O as the starting material and succeeded in synthesizing four new carboxylate-functionalized arsenomolybdates **1–4**. The reactions generally occur in a straightforward manner, in which the Mo/As/COO ratio in the product is corresponding to the reagent ratio. Compounds **1–4** have been prepared by a simple one-pot reaction of (NH<sub>4</sub>)<sub>6</sub>Mo<sub>7</sub>O<sub>24</sub>·4H<sub>2</sub>O, As<sub>2</sub>O<sub>3</sub>, and carboxylate ligands with the ratio Mo/As/{COO} = 6:1:3 in aqueous solution at 70 °C for 2 h. Crystals of **1–4** are easily converted to powders on exposure to air due to weathering. In all cases, the material As<sub>2</sub>O<sub>3</sub> suspends in the fluids and the solutions turn yellow (brown for **1**) after reacting about 2 h in a water bath. In addition, the yield of **1** is lower than **2–4**, probably because a great quantity precipitate has been obtained for **1** after the resultant solution cooled to room temperature. IR spectrum confirmed the precipitate is the powder of **1**. As is known, 1,3,5-benzenetricarboxylic acid is difficult to dissolve in water; therefore, we have to change our strategy to synthesize **4**. 1,3,5-Benzenetricarboxylic acid (BTC) has been dissolved into sodium hydroxide solution with a molar ratio of 1/3. As expected, the BTC ligands substitute oxo groups of the POMs and are directly linked to the molybdenum centers. Preparation of **4** perhaps opens a new perspective, suggesting the solubility of carboxylic acid plays an important role in the assembly of covalent system.

**Structure of the Anions.** All crystallographic data of the four compounds reported here are gathered in Table 1. Single-crystal X-ray analyses confirm that all four compounds contain

the common {AsMo<sub>6</sub>} unit (Figure S1, Supporting Information), which consists of a ring of six nearly coplanar corner- and edge-sharing MoO<sub>6</sub> octahedra. In this unit, the central As atom connects to the ring through three μ<sub>3</sub>-O atoms and is located slightly above the plane of the {Mo<sub>6</sub>} ring, presenting a trigonal-pyramidal coordination geometry. This flat arrangement of the {AsMo<sub>6</sub>} unit is similar to the {Ni<sub>6</sub>} cluster and Anderson-type POMs.<sup>5</sup> Besides, the six terminal oxygen atoms on one face of the {AsMo<sub>6</sub>} unit are potential reactive sites that might be substituted by the oxygen-containing ligands. Thus, we introduced a variety of carboxylate ligands into the POM frameworks. Moreover, the {AsMo<sub>6</sub>} cluster cannot be isolated and is only stable in the presence of carboxylic acids. Then it seems reasonable to infer that carboxylate ligands not only direct the assemblies of POM clusters but also have a positive effect on their stabilization. As expected, addition of different carboxylic acids resulted in a series of novel architectures generating monomer, dimer, trimer, and tetramer.

In anion **1** (Figure 2a), three *m*-aminobenzoic acid ligands, having the symmetric bidentate coordination mode, are bound to two edge-sharing MoO<sub>6</sub> octahedra via their carboxyl groups on the same side of the {Mo<sub>6</sub>} ring. As a result, the [AsMo<sub>6</sub>O<sub>21</sub>]<sup>3-</sup> unit has six anchoring points. The similar molybdenum-oxo frameworks have been observed before in the carboxylate ligands functionalized polymolybdates, [AsMo<sub>6</sub>O<sub>21</sub>(O<sub>2</sub>CC<sub>6</sub>H<sub>4</sub>NH<sub>3</sub>)<sub>3</sub>]<sup>3-</sup>,<sup>2j</sup> [Cu-(H<sub>2</sub>O)<sub>4</sub>[AsMo<sub>6</sub>O<sub>21</sub>(OAc)<sub>3</sub>]<sub>2</sub>]<sup>10-</sup>,<sup>6</sup> [(SeMo<sub>6</sub>O<sub>21</sub>)-(CH<sub>3</sub>CO<sub>2</sub>)<sub>3</sub>]<sup>3-</sup>,<sup>4e</sup> and [HPMo<sub>6</sub>O<sub>21</sub>(O<sub>2</sub>CC<sub>6</sub>H<sub>4</sub>OH)<sub>3</sub>]<sup>5-</sup>,<sup>4d</sup> which have been anchored by acetate, amino acid, and *p*-hydroxybenzoic acid. The lone pair of the arsenic atom is on the same side of the ring as carboxylate ligands. Meanwhile, it is evident that the structures functioned by monocarboxylate ligands all exhibit a monomer arrangement. To find more complicated carboxylate-functionalized heteropolyanions, we conducted a similar one-pot reaction with malonic acid substituting for *m*-aminobenzoic acid. The change of the carboxylic acid has a strong influence on the structure of **2**.



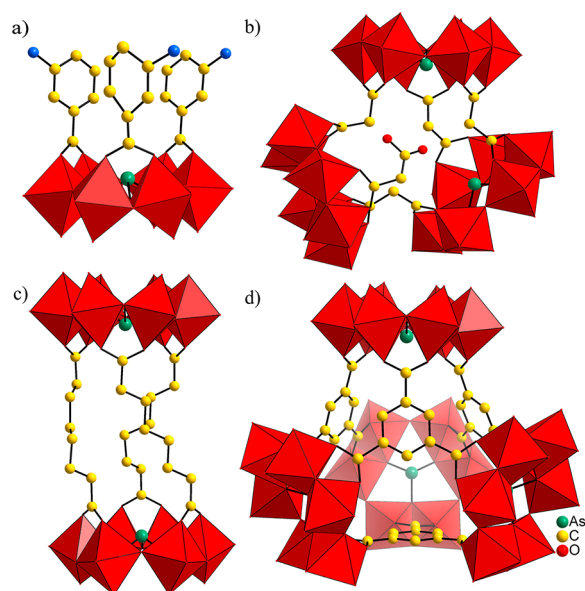


**Figure 2.** Ball-and-stick/polyhedral representation of compounds 1 (a), 2 (b), 3 (c), and 4 (d) ( $\text{MoO}_6$  octahedra red.  $\text{NH}_4^+$ ,  $\text{H}_2\text{O}$ , and hydrogen atoms are omitted for clarity).

From Figure 2b it can be seen that anion 2 is trimeric. Such an asymmetric unit consists of three  $[\text{AsMo}_6\text{O}_{21}]^{3-}$  clusters linked by five malonic acid groups, giving the anion a cage structure with gaps. Arising from the high flexibility of the malonic acid, each malonic acid linker presents a V-type and joins two  $[\text{AsMo}_6\text{O}_{21}]^{3-}$  units. On the other hand, the lone pair of the arsenic atom seems to play an important structure-controlling role in the polyanions. The structure of anion 2 is different from the  $\{\text{PMo}_6\}$  unit functionalized by malonic acid, which affords a hybrid cage with an inner cavity diameter of approximately 5.8 Å.<sup>4d</sup> In addition,  $\{\text{COO}\}$  groups are orientated almost perpendicular to the  $\{\text{AsMo}_6\}$  plane. We also observed little crystallographic disorder of one benzene ring of *m*-aminobenzoic acid in anion 1. Obviously, the steric hindrance leads to one bare carboxyl group of malonic acid in anion 2.

Actually, it is well known that the nature of carboxylic acids has a profound effect on constructing POM-based architectures. Then we explored using the more flexible ligand suberic acid in the assembly of compound 3 under the same reaction condition. To our surprise, simple extension of carboxylic acid affects formation of the structural framework. It is very interesting to note that dimer 3 can be visualized as the linkage of two  $[\text{AsMo}_6\text{O}_{21}]^{3-}$  units by three suberic acid linkers (Figure 2c). Both  $[\text{AsMo}_6\text{O}_{21}]^{3-}$  units appear nearly superimposed, and three linkers act as pillars within the scaffold structure. As a consequence of the screwed torsion, two  $\{\text{AsMo}_6\text{O}_{21}\}$  planes are slightly staggered due to the high flexibility of the suberic acids with the quite closed angle (about 2.2°). Furthermore, this result has a similar variation trend with the  $\{\text{SeMo}_6\}$  unit functionalized by  $\text{HO}_2\text{C}(\text{CH}_2)_n\text{CO}_2\text{H}$  ( $n = 0, 2, 4, 6$ ), which also shows that the dimeric motif can be formed with two carboxyl groups at the same sides of linear aliphatic chain.<sup>4c</sup>

The accessibility of 2 and 3 affords us the motivation to exploit the structural diversity for construction of hybrid cages and capsules and prompted us to use tricarboxylic acids. Functionalization with rigid ligands can allow POM clusters to be used in preparing well-defined cavities for gas storage,

separation, and catalysis.<sup>7</sup> Although the  $\{\text{PMo}_6\}$  cluster functionalized by 1,3,5-benzenetricarboxylic acid (BTC) has been reported by us,<sup>4d</sup> it is still a big challenge to experimentally control the composition of the final product. To better understand the influence of ligand solubility in this system, a stepwise approach has been adopted in the assembly process of compound 4. When BTC was completely dissolved in the solution, a POM–organic cage 4 constructed from four  $[\text{AsMo}_6\text{O}_{21}]^{3-}$  units and linkers was obtained. The coordination mode of  $\{\text{AsMo}_6\text{O}_{21}\}$  with BTC is shown in Figure 2d. Three BTC ligands covalently coordinate to three  $[\text{AsMo}_6\text{O}_{21}]^{3-}$  units through carboxyl groups. Thus, both the  $\{\text{AsMo}_6\text{O}_{21}\}$  cluster and BTC act as the three-connected units. It is striking that four  $[\text{AsMo}_6\text{O}_{21}]^{3-}$  units through four BTC coordination delimit a large hydrophilic hole (Figure 3) lined by the 24 carbon atoms of the four BTC ligands with an inner cavity diameter of approximately 8.5 Å. The large inner volume (about 320 Å<sup>3</sup>) contains 2.5 water molecules.

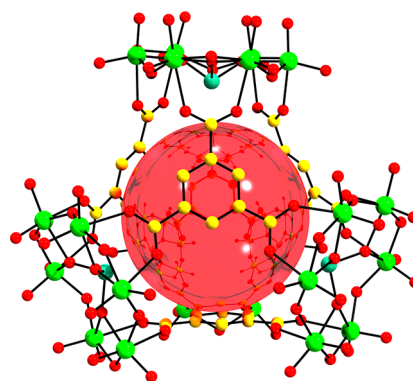


**Figure 3.** Structure of the molecular cage in 4 (color code: Mo = bright green spheres; C = yellow spheres; O = red spheres; As = green spheres.  $\text{NH}_4^+$ ,  $\text{H}_2\text{O}$ , and hydrogen atoms are omitted for clarity).

**XPS Analyses and XRPD Patterns.** The bond valence sum (BVS) calculations of 1–4 indicate that the oxidation states of all As atoms are +3,<sup>8</sup> which are further confirmed by XPS spectra (Figure S2, Supporting Information). The XPS spectra of 1–4 for As atoms exhibit two peaks with binding energies of 40.2 and 43.6 eV for 1, 40.4 and 43.6 eV for 2, 40.2 and 43.8 eV for 3, and 40.2 and 44.0 eV for 4, attributed to  $\text{As}^{3+}$  ( $3d_{5/2}$ ) and  $\text{As}^{3+}$  ( $3d_{3/2}$ ), respectively.<sup>9</sup> The purity of the phases has been checked by comparison of the experimental X-ray powder pattern with the powder pattern calculated from the structure solved from single-crystal X-ray diffraction data (Figure S3, Supporting Information).

**FT-IR Spectroscopy.** Infrared spectra of 1–4 (Figure S4, Supporting Information) show similar characteristic peaks for the skeletal vibrations in the region between 450 and 1650  $\text{cm}^{-1}$ , indicating 1–4 almost have the same basic framework, which are in good agreement with the results of single-crystal X-ray structural analyses. In comparison with the uncoordinated acid (1700–1740  $\text{cm}^{-1}$ ), the  $\nu_{\text{COO}}$  vibrations of 1–4 are shifted to low frequency as a result of the carboxylate interaction with metal ion,<sup>2c</sup> indicating the grafting of organic ligands onto the surface of POMs. The  $\text{Mo}=\text{O}$  stretching vibrations are identified around 930, 918, and 891  $\text{cm}^{-1}$  for 1, 933, 916, and 889  $\text{cm}^{-1}$  for 2, 930, 912, and 892  $\text{cm}^{-1}$  for 3, and 935 and 890  $\text{cm}^{-1}$  for 4. More specifically, the  $\nu(\text{Mo}-\text{O}-\text{Mo})$  bands appear in the region 771–669  $\text{cm}^{-1}$ , leading to an

overlap with the  $\nu(\text{As}-\text{O})$  stretching vibration bands.<sup>9b,c</sup> The bands at  $3531\text{--}3034\text{ cm}^{-1}$  with strong strength are probably because of the stretching vibrations  $\nu(\text{H}-\text{O})$  and  $\nu(\text{N}-\text{H})$ .

**Thermogravimetric Analyses (TGA).** The thermal decomposition process of **2** is approximately divided into three steps (Figure S5a, Supporting Information). The first weight loss of 13.31% from 25 to 197 °C is comparable with the calculated value of 14.61%, corresponding to the loss of 18 lattice water and 16  $\text{NH}_3$  molecules. The residual weight loss at this temperature range is slightly higher than expected for the stoichiometric amount, which probably is because these crystals easily lose solvent molecules in air. The second weight loss of 28.34% between 197 and 433 °C is ascribed to the escaping of three coordination water molecules, five malonate ligands, and arsenic oxides (calcd 21.32%). Here the residual weight loss at this temperature range is considerably lower than expected for the stoichiometric amount, which is caused by the reduction of POMs. The third loss at 433–800 °C corresponds to sublimation of metal oxides.

The TGA curve of **3** is shown in Figure S5b, Supporting Information. There is a one-slow-step decomposition between 25 and 800 °C. The weight loss 53.41% is attributed to release of 8 lattice water molecules, 11  $\text{NH}_3$  molecules, 1 coordination water molecule, 3 suberate ligands, and arsenic oxides and sublimation of metal oxides.

The TGA trace for **4** also shows a gradual decomposition over the temperature range 25–800 °C, without well-defined decomposition steps (Figure S5c, Supporting Information). The total weight loss of 48.94% can be assigned to removal of the 24-point five lattice water molecules, 18  $\text{NH}_3$  molecules, 6 coordination water molecules, 4 1,3,5-benzenetricarboxylate ligands, and arsenic oxides and sublimation of metal oxides.

**EPR and XPS Spectroscopy.** It is very interesting to find that heating of powders **1–4** induced obvious color changes, and the colors gradually shifted to blue with a high coloration contrast. Dark blue powders **2** and **3** are soluble in water after heating at 453 K for 0.5 h, and the color of sample solutions is deep blue. In contrast, **1** and **4** show slow coloration changes (which are light blue at 453 K) and cannot dissolve completely in water. The color changes may be due to reduction of the POMs. Formation of reduced metallic centers in **2** can be well evidenced by EPR spectroscopy. The reduced sample of **2** exhibits a significant paramagnetic signal at 298 K, attributed to  $\text{Mo}^{5+}$  with  $g = 1.923$  (Figure 4).<sup>10</sup> Moreover, the XPS spectrum, illustrated in Figure 5a, displays two well-resolved spectral lines at 235.1 and 231.9 eV, which are assigned to  $\text{Mo}^{\text{V}} 3d_{3/2}$  and  $\text{Mo}^{\text{V}} 3d_{5/2}$ , respectively.<sup>11</sup> Although XPS spectroscopy is a surface analysis technique, the presence of  $\text{Mo}(\text{V})$  at the surface is circumstantial evidence in the reduced sample. While the spectrum of the reduced sample in the As 3d region shows a

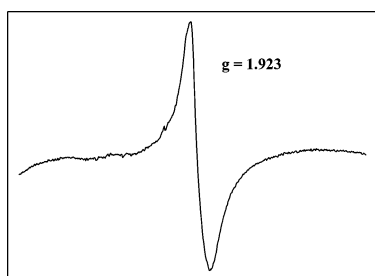


Figure 4. EPR spectrum of **2** after heating at 453K for 7 h.

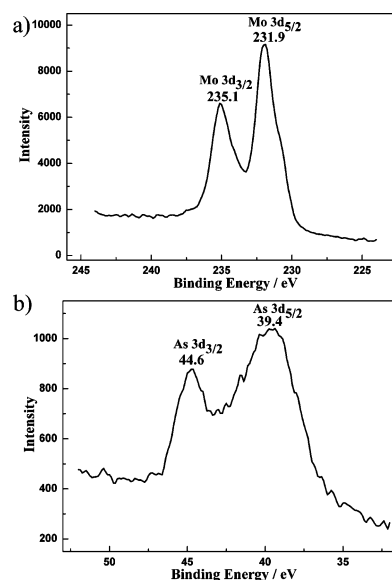


Figure 5. (a) XPS spectrum of reduced sample **2** for Mo 3d; (b) XPS spectrum of reduced sample **2** for As 3d.

binding energy at 44.6 and 39.4 eV (Figure 5b), attributed to  $\text{As}^{\text{V}}$ .<sup>9c</sup>

## CONCLUSION

In summary, we designed and developed a modular synthetic approach to incorporate carboxylic acids into arsenomolybdates. Structural characterization of compounds **1–4** reveals that configurable design of these hybrids is mainly governed by the inherent nature of carboxylic acids, simultaneously highlighting the structure-directing role of carboxylate linkers in the polyoxoanion self-assembly processes. Successful preparation of these POMs provides a simple, a cheap, and an efficient synthetic route for covalent grafting of organic groups onto POM cluster and further guides the rational conformational design of the inorganic–organic frameworks based on the inherent nature of addenda ligands. Currently, we are in the process of preparing high-dimensional POMs derivatives using other carboxylic acids. Interestingly, we discovered that when the carboxylic acids were  $\text{HO}_2\text{C}-(\text{CH}_2)_n\text{CO}_2\text{H}$  ( $n = 0, 2, 4$ ), dimers similar to **3** were obtained. This discovery proves that the carboxylic acids act not simply as ligands but also as structure-directing agents.

## ASSOCIATED CONTENT

### Supporting Information

Figures S1–S7. This material is available free of charge via the Internet at <http://pubs.acs.org>.

## AUTHOR INFORMATION

### Corresponding Authors

\*E-mail: [jpwang@henu.edu.cn](mailto:jpwang@henu.edu.cn).

\*E-mail: [jyniu@henu.edu.cn](mailto:jyniu@henu.edu.cn).

### Notes

The authors declare no competing financial interest.

## ACKNOWLEDGMENTS

The authors thank the National Natural Science Foundation of China, the Foundation of Education Department of Henan

Province, and the Natural Science Foundation of Henan Province for financial support.

## REFERENCES

- (1) (a) Gouzerh, P.; Proust, A. *Chem. Rev.* **1998**, *98*, 77–111. (b) Dolbecq, A.; Dumas, E.; Mayer, C. R.; Mialane, P. *Chem. Rev.* **2010**, *110*, 6009–6048. (c) Miras, H. N.; Yan, J.; Long, D. L.; Cronin, L. *Chem. Soc. Rev.* **2012**, *41*, 7403–7430. (d) Müller, A.; Gouzerh, P. *Chem. Soc. Rev.* **2012**, *41*, 7431–7463. (e) Banerjee, A.; Bassil, B. S.; Rösenthaller, G.-V.; Kortz, U. *Chem. Soc. Rev.* **2012**, *41*, 7590–7604. (f) Proust, A.; Matt, B.; Villanneau, R.; Guillemot, G.; Gouzerha, P.; Izzet, G. *Chem. Soc. Rev.* **2012**, *41*, 7605–7622.
- (2) (a) Inoue, M.; Yamase, T. *Bull. Chem. Soc. Jpn.* **1995**, *68*, 3055–3063. (b) Modéc, B.; Brenčić, J. V.; Dolenc, D.; Zubieta, J. *Dalton Trans.* **2002**, 4582–4586. (c) Modéc, B.; Dolenc, D.; Kasunič, M. *Inorg. Chem.* **2008**, *47*, 3625–3633. (d) Cadot, E.; Sécheresse, F. *Chem. Commun.* **2002**, 2189–2197. (e) Salignac, B.; Riedel, S.; Dolbecq, A.; Sécheresse, F.; Cadot, E. *J. Am. Chem. Soc.* **2000**, *122*, 10381–10389. (f) Lemonnier, J.-F.; Floquet, S.; Marrot, J.; Terazzi, E.; Piguet, C.; Lesot, P.; Pinto, A.; Cadot, E. *Chem.—Eur. J.* **2007**, *13*, 3548–3557. (g) du Peloux, C.; Mialane, P.; Dolbecq, A.; Marrot, J.; Sécheresse, F. *Angew. Chem., Int. Ed.* **2002**, *41*, 2808–2810. (h) Yang, W. B.; Lu, C. Z.; Lin, X.; Zhuang, H. H. *Inorg. Chem.* **2002**, *41*, 452–454. (i) Zhou, Z. H.; Hou, S. Y.; Cao, Z. X.; Tsai, K. R.; Chow, Y. L. *Inorg. Chem.* **2006**, *45*, 8447–8451. (j) Kortz, U.; Savelieff, M. G.; Abou Ghali, F. Y.; Khalil, L. M.; Maalouf, S. A.; Sinno, D. I. *Angew. Chem., Int. Ed.* **2002**, *41*, 4070–4073. (k) Kortz, U.; Vaissermann, J.; Thouvenot, R.; Gouzerh, P. *Inorg. Chem.* **2003**, *42*, 1135–1139. (l) Cindrić, M.; Strukan, N.; Devčić, M.; Kamenar, B. *Inorg. Chem. Commun.* **1999**, *2*, 558–560.
- (3) (a) Liu, G.; Zhang, S. W.; Tang, Y. Q. *Z. Anorg. Allg. Chem.* **2001**, *627*, 1077–1080. (b) Modéc, B.; Brenčić, J. V.; Burkholder, E. M.; Zubieta, J. *Dalton Trans.* **2003**, 4618–4625. (c) He, X.; Ye, J. W.; Xu, J. N.; Fan, Y.; Wang, L.; Zhang, P.; Wang, Y. J. *Mol. Struct.* **2005**, *749*, 9–12. (d) Modéc, B.; Dolenc, D.; Brenčić, J. V.; Koller, J.; Zubieta, J. *Eur. J. Inorg. Chem.* **2005**, 3224–3237. (e) Cindrić, M.; Novak, T. K.; Kraljević, S.; Kralj, M.; Kamenar, B. *Inorg. Chim. Acta* **2006**, *359*, 1673–1680. (f) Lemonnier, J.-F.; Floquet, S.; Kachmar, A.; Rohmer, M.-M.; Bénard, M.; Marrot, J.; Terazzi, E.; Piguet, C.; Cadot, E. *Dalton Trans.* **2007**, 3043–3054. (g) Cartuyvels, E.; Van Hecke, K.; Van Meervelt, L.; Görrler-Walrand, C.; Parac-Vogt, T. N. *J. Inorg. Biochem.* **2008**, *102*, 1589–1598. (h) Gao, G. G.; Xu, L.; Qu, X. S.; Liu, H.; Yang, Y. Y. *Inorg. Chem.* **2008**, *47*, 3402–3407. (i) Müller, A.; Das, S. K.; Kuhlmann, C.; Bögge, H.; Schmidtman, M.; Diemann, E.; Krickemeyer, E.; Hormes, J.; Modrow, H.; Schindler, M. *Chem. Commun.* **2001**, 655–656. (j) Lemonnier, J.-F.; Kachmar, A.; Floquet, S.; Marrot, J.; Rohmer, M.-M.; Bénard, M.; Cadot, E. *Dalton Trans.* **2008**, 4565–4574. (k) Liu, G.; Zhang, S. W.; Tang, Y. Q. *J. Chem. Soc., Dalton Trans.* **2002**, 2036–2039.
- (4) (a) Zheng, S. T.; Zhang, J.; Yang, G. Y. *Angew. Chem., Int. Ed.* **2008**, *47*, 3909–3913. (b) Breen, J. M.; Schmitt, W. *Angew. Chem., Int. Ed.* **2008**, *47*, 6904–6908. (c) Marrot, J.; Pilette, M. A.; Haouas, M.; Floquet, S.; Taulelle, F.; López, X.; Poblet, J. M.; Cadot, E. *J. Am. Chem. Soc.* **2012**, *134*, 1724–1737. (d) Yang, D. H.; Li, S. Z.; Ma, P. T.; Wang, J. P.; Niu, J. Y. *Inorg. Chem.* **2013**, *52*, 8987–8992. (e) Yang, D. H.; Li, S. Z.; Ma, P. T.; Wang, J. P.; Niu, J. Y. *Inorg. Chem.* **2013**, *52*, 14034–14039.
- (5) (a) Zheng, S. T.; Zhang, J.; Li, X. X.; Fang, W. H.; Yang, G. Y. *J. Am. Chem. Soc.* **2010**, *132*, 15102–15103. (b) Wu, P. F.; Yin, P. C.; Zhang, J.; Hao, J.; Xiao, Z. C.; Wei, Y. G. *Chem.—Eur. J.* **2011**, *17*, 12002–12005.
- (6) Li, L. L.; Liu, B.; Xue, G. L.; Hu, H. M.; Fu, F.; Wang, J. W. *Cryst. Growth Des.* **2009**, *9*, 5206–5212.
- (7) (a) Kitagawa, S.; Kitaura, R.; Noro, S. *Angew. Chem.* **2004**, *116*, 2388–2430; *Angew. Chem., Int. Ed.* **2004**, *43*, 2334–2375. (b) Nohra, B.; Moll, H. E.; Albelo, L. M. R.; Mialane, P.; Marrot, J.; Mellot-Draznieks, C.; O’Keeffe, M.; Biboum, R. N.; Lemaire, J.; Keita, B.; Nadjjo, L.; Dolbecq, A. *J. Am. Chem. Soc.* **2011**, *133*, 13363–13374.
- (8) Brown, I. D.; Altermatt, D. *Acta Crystallogr.* **1985**, *B41*, 244–247.
- (9) (a) Sun, C. Y.; Li, Y. G.; Wang, E. B.; Xiao, D. R.; An, H. Y.; Xu, L. *Inorg. Chem.* **2007**, *46*, 1563–1574. (b) Zhang, Y. P.; Li, L. L.; Sun, T.; Liu, B.; Hu, H. M.; Xue, G. L. *Inorg. Chem.* **2011**, *50*, 2613–2618. (c) Niu, J. Y.; Hua, J. A.; Ma, X.; Wang, J. P. *CrystEngComm* **2012**, *14*, 4060–4067.
- (10) Baffert, C.; Boas, J. F.; Bond, A. M.; Kçgerler, P.; Long, D. L.; Pilbrow, J. R.; Cronin, L. *Chem.—Eur. J.* **2006**, *12*, 8472–8483.
- (11) (a) Ilangovan, G.; Pillai, K. C. *Langmuir* **1997**, *13*, 566–575. (b) Chen, Y. F.; Yu, G. S.; Li, F. *Inorg. Chem.* **2013**, *52*, 7431–7440.